sciendo

DOI: 10.2478/eces-2021-0029 ECOL CHEM ENG S. 2021;28(3):429-447

Mir Mehrdad MIRSANJARI[1], Jurate SUZIEDELYTE VISOCKIENE[2*]
Fatemeh MOHAMMADYARI[1] and Ardavan ZARANDIAN[3]

MODELLING OF EXPANSION CHANGES OF VILNIUS CITY AREA AND IMPACTS ON LANDSCAPE PATTERNS USING AN ARTIFICIAL NEURAL NETWORK

Abstract: The present study aimed to analyse changes in the land cover of Vilnius city and its surrounding areas and propose a scenario for their future changes using an Artificial Neural Network. The land cover dynamics modelling was based on a multilayer perceptron neural network. Landscape metrics at a class and landscape level were evaluated to determine the amount of changes in the land uses. As the results showed, the Built-up area class increased, while the forest (Semi forest and Dense forest) classes decreased during the period from 1999 to 2019. The predicted scenario showed a considerable increase of about 60 % in the Built-up area until 2039. The vegetation plant areas consist about 47 % of all the area in 2019, but it will be 36 % in 2039, if this trend (urban expansion) continues in the further. The findings further indicated the major urban expansion in the vegetation areas. However, Built-up area would expand over Semi forest land and Dense forest land, with a large part of them changed into built- up areas.

Keywords: land cover, land change modeller, Artificial Neural Network, Markov chain, urban expansion, landscape patterns

Introduction

Today, about 55 % of the people of the world live in urban areas, while it was only 30 % in 1950. A study found that this figure will amount to 68 % by 2050 [1]. Therefore, the increased density of most cities and expansion of their areas beyond the outer boundaries destroy natural spaces such as forests or bodies of water [2]. The global pervasiveness of land cover change, predominantly as a result of human use, has created concerns about the sustainability and consequences of current land use trends, which in turn has led to the emergence of land change science [3]. Anthropogenic utilization of land is known as ‘land use’ and unaltered surfaces are described as areas with a land cover [4]. Urban expansion is a land use change process that converts non-urban land to urban land as well as a major driver of changes in the local to global land cover [5, 6]. Urban sprawl leads to land-use/land-cover changes [7] such as loss and fragmentation of forest and farmland

[1] Department of Environmental Sciences, Malayer University, Malayer, Iran, email: mmirsanjari@malayeru.ac.ir, m.fatima.1364@gmail.com, ORCID: MMM 0000-0002-5968-4422, FM 0000-0002-8126-9807
[2] Department of Geodesy and Cadastre, Vilnius Gediminas Technical University, Sauletekio al. 11, LT-10223 Vilnius, Lithuania, phone +37060607799, email: jurate.visockiene@vgtu.lt, ORCID: 0000-0001-9764-8476
[3] Group of Environmental Assessment and Risks, Researcher Center for Environmental and Sustainable Development (RCESD), Tehran, Iran email: azarandian@gmail.com, ORCID: 0000-0002-7099-9839
[*] Corresponding author: jurate.visockiene@vgtu.lt

[8], which imposes considerable stress on ecosystems [7]. In fact, Urban expansion have irreversible impacts on local communities and landscapes [9]. Rapid changes in urban land use together with economic development has increased the demand for urban spaces and created growing serious environmental problems [10]. Besides providing economic opportunities and improving the quality of life, urbanization has negative consequences such as [11], climate change [12], intensified urban heat island effects [13], air pollution [14], soil pollution [15] and water pollution [16]. Population growth, economic development, urbanization, industrial restructuring, natural geographical environment or land use policies are the factors affecting urban expansion [17]. From among these factors, economic development, demographic changes and urbanization are considered to be the main drivers of urban expansion [18]. Land-use change has attracted the attention of managers and planners who are engaged in the issues related to sustainable urban and environmental development [19]. Therefore, determination of recent changes in land use and knowing how these changes will happen are of great importance [20]. Different types of land use can be measured by landscape pattern analysis which gives useful information about land use changes [7]. Furthermore, the configuration, fragmentation, and complexity of the urban landscape can be determined by using landscape pattern indicators [19]. Landscape indices can objectively and directly act as strong quantitative descriptors of the structure and spatial patterns of a city [21]. Therefore, land use changes should be detected through Landscape pattern analysis [7]. Recently, research on urban growth and landscape changes has attracted increasing attention [7, 9, 11, 12, 15, 19, 21-31]. Remote sensing (*RS*) data which are processed by geographic information system (*GIS*) software have been known as a very useful tool in studies on land use, especially for detection, mapping and modelling land cover patterns in a given area over a specific period of time [32]. The evolution in the use of *RS* and *GIS* the past two decades, has led to the application of new spatial modelling approaches such as artificial neural networks (*ANN*) and cellular automata [30]. The highly sophisticated "collective behaviour" of *ANN* has made it possible for them to be employed in complex domains such as land use changes [32], as many studies have used them to model land use/cover changes [3, 26, 33-35].

This study is the first applicable study in the utilization of Landscape patterns in Vilnius city and its surrounding areas of Lithuania, where urban expansion has changed the Landscape patterns. The innovation of the present study is the evaluation of urban expansion on Landscape patterns in addition to the basic (1999) and current (2019) scenarios in the future scenario (2039). The present study aims at (i) using the Landsat imagery to prepare land use-cover (*LULC*) maps for 1999 and 2019; (ii) assessing Land use changes on the basis of land change Modular (*LCM*) for the period from 1999 to 2019, (iii) predicting the plausible land cover pattern in the Vilnius city area using an algorithm based on *ANN* for 2039; and (iiii) Evaluating and modelling the effects of urban expansion on Landscape Patterns in 1999, 2019 and 2039 scenarios.

Materials and methods

Location and description of the study area

The studied region consists of Vilnius city and the surrounding area, which occupy an area of 133.3 km^2, located between 54°38′-54°45′ N of latitude and 25°12′-25°22′ E of longitude (Fig. 1). Vilnius, the capital of Lithuania and its largest city is located at the confluence of the Vilnia and Neris Rivers [36].

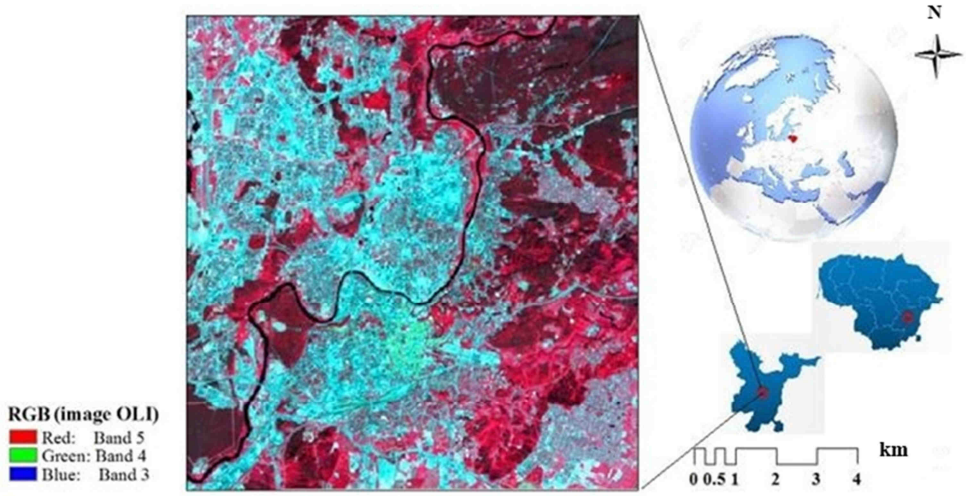


Fig. 1. Geographical location of Vilnius city and the surrounding area

Data sources and processing

The current study applied the Landsat images from Operational Land Imager (*OLI*) sensor and Thematic Mapper (*TM*) sensor to prepare the base maps for analysis purpose from the USGS official website [37]. The satellite images for 1999 and 2019 were selected. *OLI* sensor (Landsat 8) is the most new production of Landsat satellite that prepares remote sensing imagery for earth observation. The *OLI* sensor contains enhanced bands due to new linear detector arrays which gather images in a push-broom scanner mode providing a superior signal with a high signal to noise proportion. The basic discrepancy between *TM* and *OLI* sensor refer to the overall image quality, to the different number of spectral bands, width and their spatial resolutions [38]. We used the *RGB* combination to better classify satellite images. The *RGB* model is an augmentative colour model in which red, green, and blue light are added each other in various ways to product a vast rank of colours. Any parameter red, green, and blue describe the severity of the colour with a value between 0 and 255 (Table 1).

To diminish the effect of the cloud cover and shadow, only the images that have a cloud cover of less than 10 % and no clouds in the study area were selected because the clouds inhibit the classification and interpretation of satellite images [34].

Table 1

Characteristics of the images used in the classification of the land cover

Date	Satellite	Sensor	Bands	Resolution [m]
05/31/1999	Landsat 5	*TM*	321 (*RGB*)	30
05/31/2019	Landsat 8	*OLI*	432 (*RGB*)	30

Images georeferencing and pre-processing were performed in *QGIS* software. The images were classified using Support Vector Machine (*SVM*) method in *ENVI* environment, which have recently been widely used by many researchers in *LULC* modeling [39, 40].

SVM considers both continuous and categorical variables, non-linear relationships, noisy and complex data, non-normally distributed data, and training datasets with outliers. It further avoids overfitting and guarantees good generalization. These characteristics have made *SVM* a very applicable tool for modeling urban expansion patterns [41]. The present study identified seven main *LULC* types of classes, including Built-up area, Cropland, Semi forest land, Dense forest land, Water bodies, Pastures and Green urban areas. Finally, some of the isolated pixels were filtered and generalized in the most common neighboring class [19]. According to Santana et al. [42], *Kappa* coefficient of agreement was used to evaluate the image classification performance [34, 42]. Which was calculated by the following formula [34]:

$$I = \frac{n\sum_{i=1}^{c} x_{ii} - \sum_{i=1}^{c} x_{i+}x_{+i}}{n^2 - \sum_{i=1}^{c} x_{i+}x_{+i}} \quad (1)$$

where: I - the *Kappa* coefficient, ii - the value in row i and column i, $x_(i+)$ - the sum of row i, $x_(+i)$ - the sum of column i of the matrix, n - the total number of observations, and c - the total number of classes indicate.

Prediction of land cover

Land cover was predicted using artificial neural network and Markov chain methods. Artificial Neural Network (*ANN*) is widely employed to predict how the output variables are dependent upon the input data sets, particularly in nonlinear systems behaviour [10, 43]. The method relied on the role of the human brain in creating connection between several neurons [43]. The present study implied Multilayer Perceptron (*MLP*) that is the most common type of *ANN* [44] which involves input, hidden, and output layers [45], such that layers process signal and search for the best linear and nonlinear relationships between input and output [46]. The layer that produces the ultimate result is the output layer. Prediction of land cover can be analysed by *ANN* model (*MLP*). To run the *MLP*, the Land Change Modular (*LCM*) module of *TerrSet* software was employed in many studies leading to satisfactory results [47]. *MLP* model was used to simulate the future scenario. *LCM* consists of a set of intelligent tools dealing with automated assessment of the habitat, resources management and the complexity of land-use change analysis [48]. *LCM* shows the tendency of changes and the pixels of the different land cover classes that persistently change. To predict the transition, the major changes in the land cover were analysed in the experimental area between 1999 and 2019 in order to define the transition classes. After defining the transition classes, explanatory variables were selected by using the Cramer test. Based on [34, 49], variables which presented Cramer values > 0.15 were considered in land cover modelling. In accordance with the changes of the land cover in the area, therefore, the following explanatory variables were selected to be tested: Digital Elevation Model (*DEM*), Slope, Euclidean distances from Built-up, Cropland, Semi forest land, Dense forest land, Water bodies, Pastures, Green urban areas and Evidence Likelihood (Fig. 2a). For Euclidean distance analysis, the raster layers were prepared in a distance from land use classes by *GIS* software.

The Cramer test takes a value between 0 and 1, and the value closer to 1 should be indicates that the explanatory variable is more associated with the defined transition classes. This test is used to evaluate the strength of the association between variables [4].

The neural network was executed after defining the transition classes. The resulting accuracy is dependent on the iteration between the explanatory variables and the considered transitions. Recommended accuracy is greater than or equal to 80 %, e.g. [4, 34].

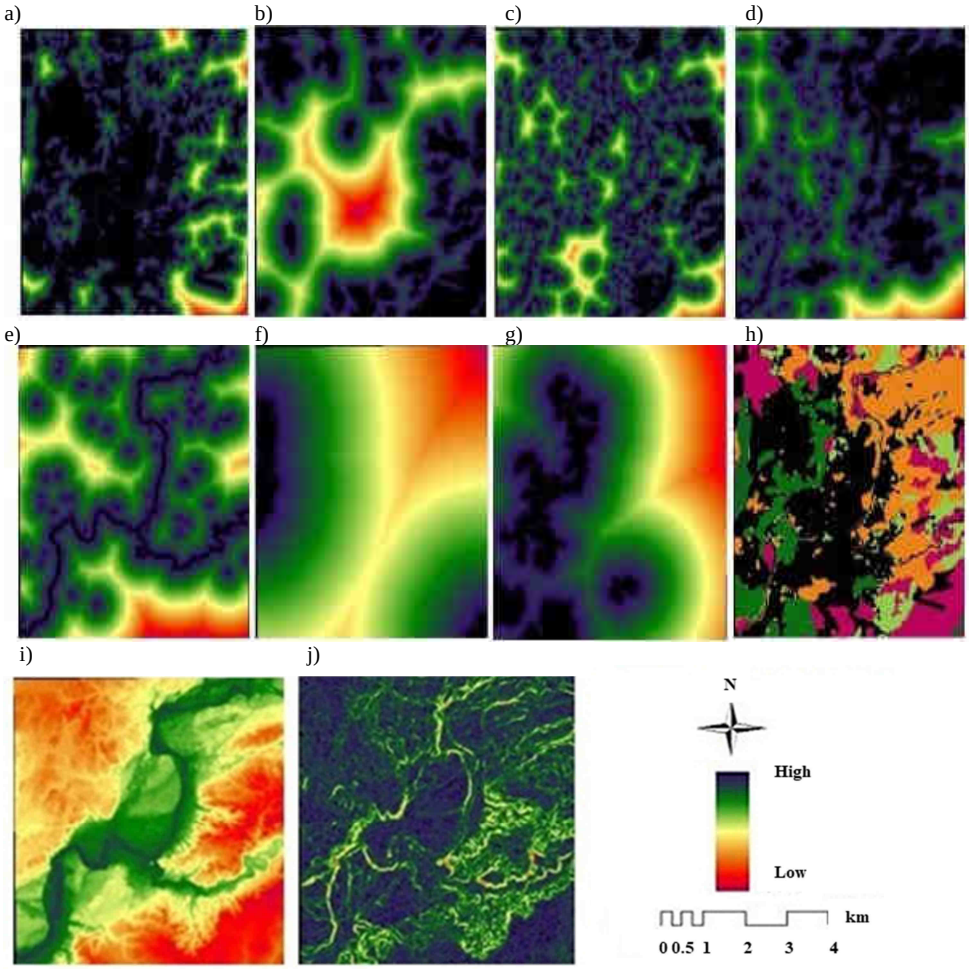


Fig. 2. Raster layers of driver variables as the continuous values: a) distances from Built-up; b) distances from Cropland; c) distances from Semi forest land; d) distances from Dense forest land; e) distances from Water bodies; f) distances from Pastures; g) distances from Green urban areas; h) Evidence Likelihood; i) *DEM*; and j) Slope

To predict *LULC* changes, Markov method was conducted within Terrset software package. The output of the *ANN* model (*MLP*) is used as the input of the Markov model. The Markov model as a stochastic model is employed to simulate the continuous surfaces that are randomly changing [42] at a time interval depending on their value at the previous time [19]. In *LULC* changes the model represents the amount of changes of land classes and computes the rates of transfer of various types of land use [47]. Therefore, it makes use of

matrices that indicates all the multi-directional *LULC* dynamics among all the mutually exclusive *LULC* types [42]. The probability matrix of transition was used to calculate the changes in *LULC*. Markov model in *LULC* changes, the model presents the amount of conversion of land classes and evaluates the rate of transfer among various types of land use [42].

Landscape approach

After providing the land cover maps, eight landscape metrics were evaluated in class and landscape level using *FRAGSTATS* 4.1 software. Landscape metrics in class level are number of patches (*NP*) that measures patch characteristics [26]:

$$NP = N_i \tag{2}$$

where N_i - number of patches in the landscape of patch type (class) *i*.

The percentage of landscape (*PLAND*) that measures the proportional abundance of each patch type in the landscape [50]:

$$PLAND = P_i = \frac{\sum_{j=1}^{n} a_{ij}}{A}(100) \tag{3}$$

where: P_i - proportion of the landscape occupied by patch type (class) *i*; a_{ij} - area [m^2] of patch *ij*; *A* - total landscape area [m^2].

Edge density (*ED*) that determines the amount of urban edges in relation to the total landscape area and indicates the contiguity of the urban landscape [21]:

$$ED = \frac{\sum_{k=1}^{m} e_{ik}}{A}(10000) \tag{4}$$

where: e_{ik} - total length [m] of edge in landscape between patch types (classes) *i* and *k*; *m* - number of patch types (classes) present in the landscape, including the landscape border, if present; *A* - total landscape area [m^2].

Interspersion Juxtaposition Index (*IJI*) that shows the number of patch types that exist in the landscape [7]:

$$IJI = \frac{-\sum_{k=1}^{m}\left[\left(\frac{e_{ik}}{\sum_{k=1}^{m} e_{ik}}\right)\ln\left(\frac{e_{ik}}{\sum_{k=1}^{m} e_{ik}}\right)\right]}{\ln(m-1)}(100) \tag{5}$$

where: e_{ik} = total length [m] of edge in landscape between patch types (classes) *i* and *k*, *m* = number of patch types (classes) present in the landscape.

Euclidean nearest neighbour distance distribution (*ENN-MN*) that is the simplest measure of patch context extensively employed to quantify patch isolation (Eq. (6)) and Largest Patch Index (*LPI*) that determine the percentage of total landscape area comprised by the largest patch (Eq. (7)).

$$ENN = h_{ij} \tag{6}$$

where: h_{ij} - distance [m] from patch *ij* to nearest neighbouring patch of the same type (class), based on patch edge-to-edge distance, computed from cell center to cell center.

$$LPI = \frac{max_{j=1}^{a}(a_{ij})}{A}(100) \tag{7}$$

Landscape metrics in landscape level include Contagion Index (*CONTAG*) that sees a mosaic of the city region as a whole [19], (Eq. (8)) and Shannon's diversity index (*SHDI*) that reflects the heterogeneity of the landscape (Eq. (9)) [31]:

$$CONTAG = \left[1 + \frac{\sum_{i=1}^{m}\sum_{k=1}^{m}\left[p_i \frac{g_{ik}}{\sum_{k=1}^{m} g_{ik}}\right].\left[\ln\left(p_i \frac{g_{ik}}{\sum_{k=1}^{m} g_{ik}}\right)\right]}{2\ln(m)}\right](100) \quad (8)$$

CONTAG approaches value is 0 when patch types are unbundled to the maximum and interleaved.

$$SHDI = -\sum_{i=1}^{m}(P_i \ln P_i) \quad (9)$$

Such metrics are appropriate variables with low correlation [23, 51] which have been applied by many authors to assess spatial-temporal changes of urban expansion [7, 19, 23, 26, 31, 51].

The approach taken in the study area presents in the Figure 3.

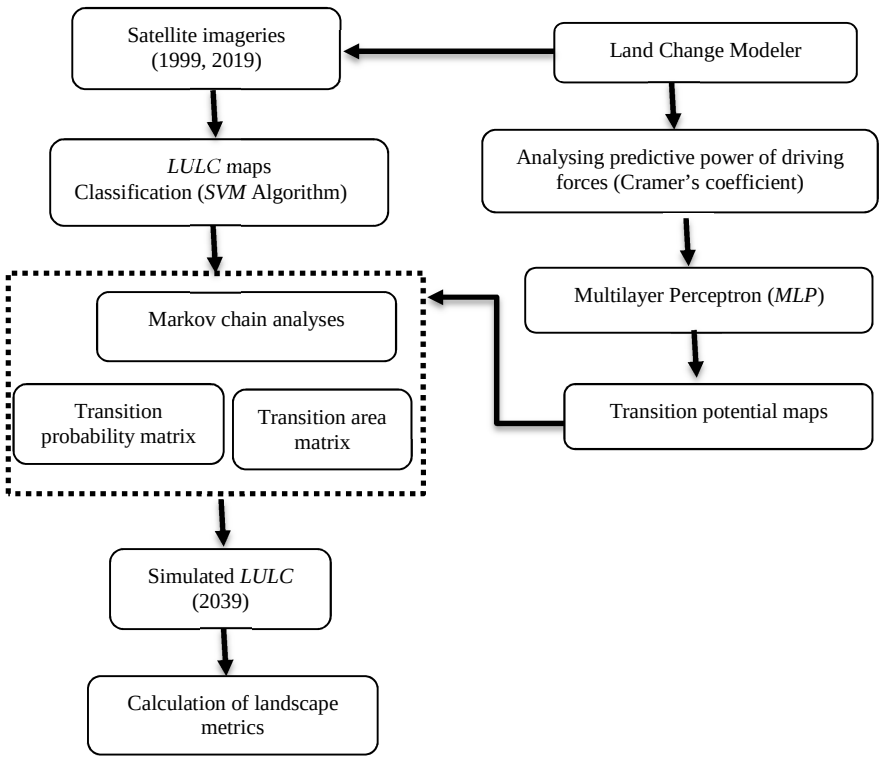


Fig. 3. Analytical framework in the study area

Results

Changes in land cover from 1999 to 2019

LUCC maps for 1999 and 2019 are shown in Figure 4. The landscape of Vilnius city has considerably changed since 20 years ago. Accordingly, the assessment of *Kappa* coefficient showed 86 and 87 % of overall accuracy and 0.91 and 0.92 of overall *Kappa* coefficient for 1999 to 2019 maps, respectively, which were acceptable results.

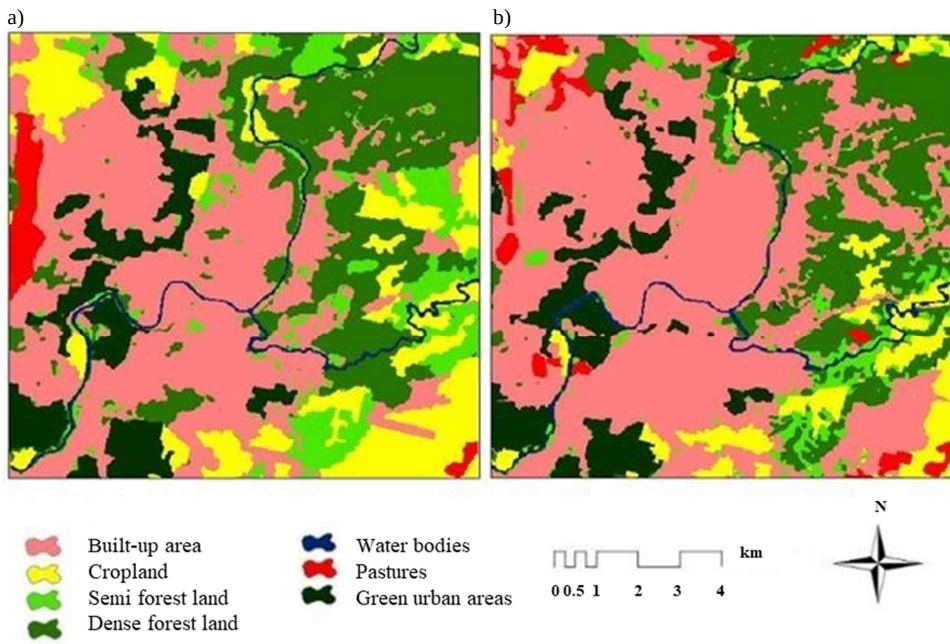


Fig. 4. The Land use map of the study area by the period of investigation: a) 1999 year; b) 2019 year

Table 2

Land cover of the Vilnius city in 1999 and 2019

Classes	Area [m^2]		Changes [m^2]	Trends
	1999 year	2019 year		
Built-up area	52.15	66.33	14.18	⇑
Cropland	18.2	11.12	–7.08	⇓
Semi forest land	14.08	7.74	–6.34	⇓
Dense forest land	31.1	29.2	–1.9	⇓
Water bodies	2.73	2.73	-	-
Pastures	2.94	4.55	1.66	⇑
Green urban areas	12.1	11.63	–0.47	⇓

The experimental area was 133.3 km^2 in whole. Built-up class had the largest area (50 %) among the classified classes. This area occupied 52.15 km^2 in 1999 and increased by 14.18 km^2 (21 %) after 20 years. In the Eastern side, Built-up area class was the most prominent class and Cropland, Semi forest land and Dense forest lands were decreasing.

However, no change was observed in the Water body class area (2.73 km^2). On the East and Northeast, a decrease was seen in Cropland, Semi forest land and Dense forest class and an increase in the Built-up area. The Pastures declined, especially in the Southwest, in comparison with 1999. The resulting land cover maps show that Green Urban areas had a decrease of only 0.47 km^2 (4 %). As it can be seen, the value is insignificant in spite of its importance in air pollution. Cropland, Semi forest, Dense forest and Green urban areas have had a declining trend during the past 20 years (Table 2).

The horizontal histogram in *LCM* shown in Figures 5 and 6 indicated the trend and amount of changes (increase and decrease) of each *LULC* type during the period from 1999 to 2019. In addition, the net change in the area of land uses for the period between 1999 and 2019 is shown in the Figure 6.

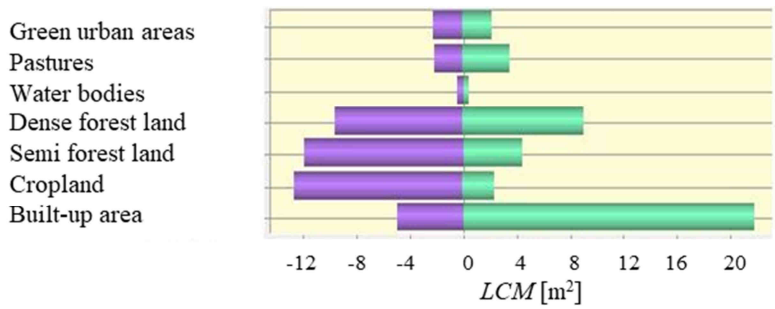


Fig. 5. Gains and losses between 1999 (colour blue) and 2019 (colour green)

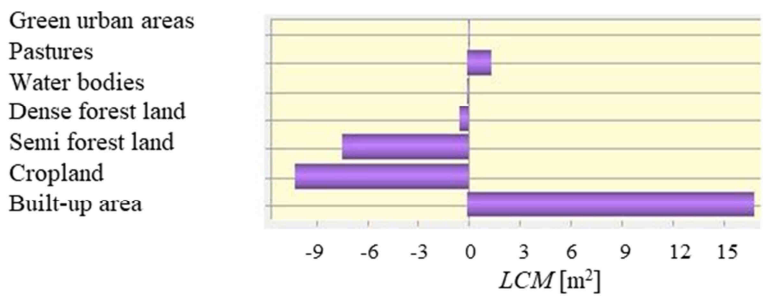


Fig. 6. Net change in land use area (1999 and 2019)

Based on the results, Built-up area reached to 21.78 km^2 in the study period. The classes (Cropland, Semi forest land and Dense forest land) had a significant decrease. For example, Cropland, Semi forest and Dense forest lands diminished about 12.67, 11.85 and 9.57 km^2, respectively. Therefore, this area is rapidly losing its environmental and biotic integrity. Destruction of green areas is a common phenomenon occurring in this region due to human intervention.

Modelling of the estimated land cover

Explanatory variables required for the land cover modelling for Vilnius city for 2039 were obtained from the Cramer's V test (Table 3). The selected variables had a correlation coefficient of more than 0.15.

Table 3

Results for the Cramer's V test for the explanatory variables

Explanatory variables [-]	Overall Cramer's
DEM [-]	0.17
Slope [-]	0.01
Distance Built-up area [-]	0.25
Distance Cropland [-]	0.19
Distance Semi forest land [-]	0.12
Distance Dense forest land [-]	0.15
Distance Water [-]	0.14
Distance Pastures [-]	0.22
Distance Green urban areas [-]	0.27
Evidence likelihood [-]	0.47

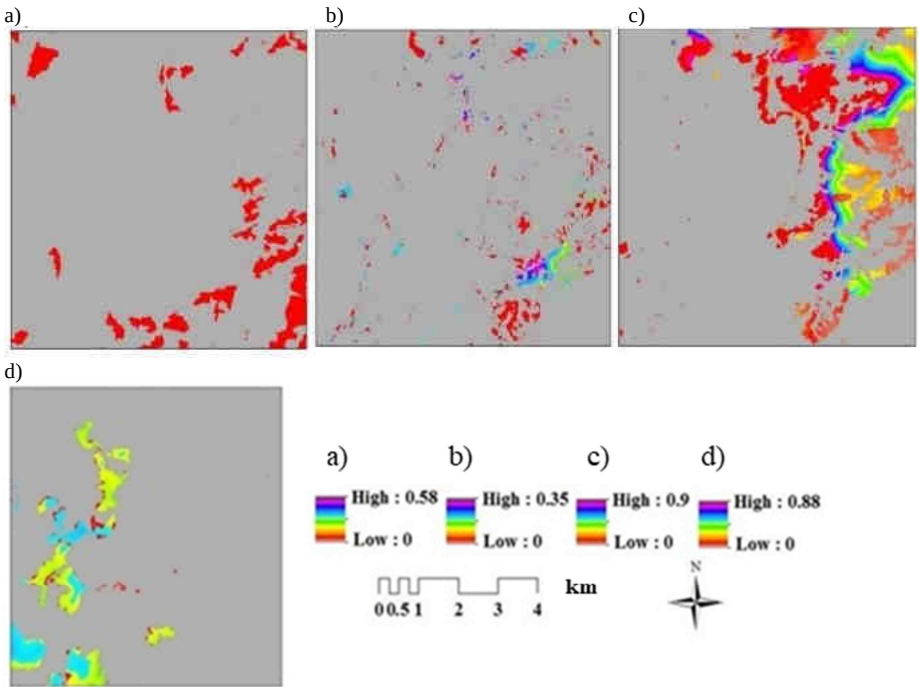


Fig. 7. Transition probability maps: a) transition probability Cropland to Built-up area; b) transition probability Semi forest land to Built-up area; c) transition probability Dense forest land to Built-up area; d) transition probability Green urban areas to Built-up area

The evidence likelihood and distance from green urban areas and Built-up areas were the most significant variables according to the Cramer V test. However, the lowest values

were obtained for the Slope variable, indicating that this variable is insignificant in predicting the land cover in the study area. To dynamically model the land cover, the best training result on the basis of *MLP* algorithm was achieved from the iteration of the explanatory variables with the transitions of interest and an accuracy rate of 85.78 %. Considering the independent variables and submodels, transition probability maps were drawn for every sub-model by using multilayer Perceptron neural networks (Fig. 7).

The next step is to calculate the Markov transition probability by Markov transitional probability matrix. The land cover transition probability matrix obtained by *MC* for 2039 is presented in Table 4.

The results of the diagonal indicate the percentages of persistence, while the other ones represent the percentages of change from one land cover category to another (Table 4). The Built-up area, Dense forest land, Water bodies and Green urban areas had a probability of persistence of more than 65 %. However, the highest amount of probability (51 %) was observed in the change from pastures to the Built-up area.

Table 4

Matrix of the transition probability of land cover categories

Classes	Built-up area	Cropland	Semi forest land	Dense forest land	Water bodies	Pastures	Green urban areas
Built-up area	0.9911	0.0129	0.0167	0.0253	0.0018	0.0148	0.0173
Cropland	0.3880	0.4340	0.0529	0.0320	0.0019	0.0832	0.0079
Semi forest land	0.2245	0.0548	0.2201	0.4286	0.0068	0.0380	0.0273
Dense forest land	0.1955	0.0156	0.0648	0.6905	0.0053	0.0097	0.0186
Water bodies	0.0445	0.0333	0.0277	0.0323	0.8519	0.0003	0.0099
Pastures	0.5123	0.0788	0.0234	0.0539	0.0000	0.3143	0.0172
Green urban areas	0.1489	0.0031	0.0114	0.0128	0.0009	0.0000	0.8229

Land cover prediction for 2039

LUCC map prediction for 2039 is shown in Figure 8.

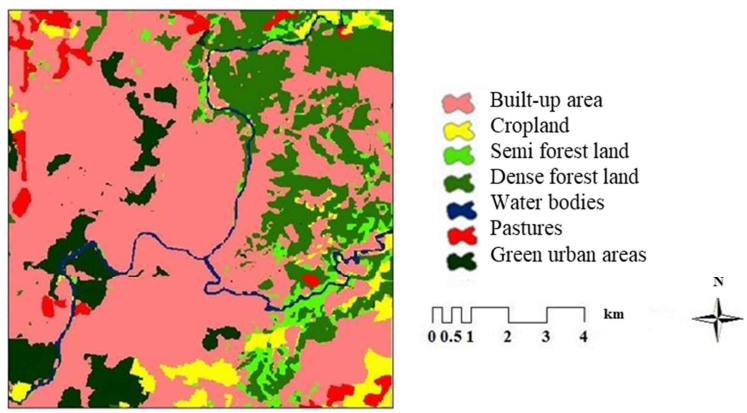


Fig. 8. Land cover prediction for 2039 for the Vilnius city

The modelling showed that the Built-up areas and Dense forest lands were the most significant areas occupying 60 % and 18 % of the whole area, respectively (Table 5).

Table 5

Land cover of the Vilnius city for year 2039

Classes	Area [km^2]
Built-up area	79.62
Cropland	6.26
Semi forest land	6.01
Dense forest land	24.03
Water bodies	2.73
Pastures	4.55
Green urban areas	10.1

Figure 9 shows the trend of changes in land cover classes in 1999, 2019 and 2039.

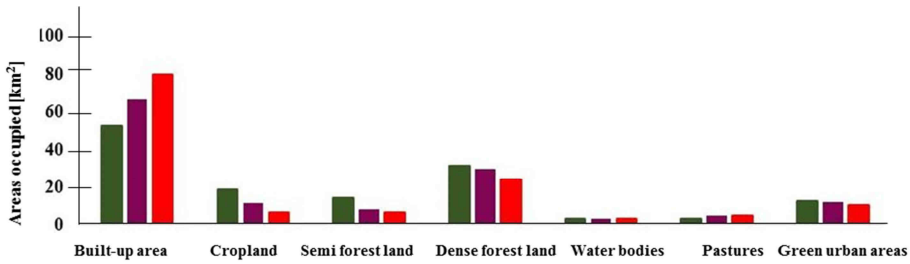


Fig. 9. Areas occupied by the land cover classes in the Vilnius city: - 1999, - 2019 and - 2039

Landscape metrics

As the values obtained for *PLAND* metric in Figure 10 showed, Built-up area, Pastures and Water bodies increased and Cropland, Semi forest land, Dense forest land and Green urban areas decreased during the period from 1999 to 2019. This trend is expected to continue in 2039.

LPI metric value increased only for Built-up area from 1999 to 2019 and decreased for other classes (Cropland, Semi forest land, Dense forest land, Water body, Pastures and Green urban areas). It was also predicted to decrease in all classes except Built-up areas in 2039. In the period from 1999 to 2039, the value of *NP* decreased in Built-up area, Semi forest land, Dense forest land and Water bodies and increased in Cropland, Pastures and Green urban areas. An increase was observed in the *IJI* value of Built-up area from 1999 to 2019. In Cropland, Semi forest land and Water bodies, the *IJI* value decreased initially and increased subsequently from 1999 to 2019. Furthermore, for Dense forest land, Pastures and Green urban areas, the *IJI* values initially increased and then decreased from 1999 to 2019. This metric was predicted to decrease in all classes except Built-up areas in 2039.

In the period from 1999 to 2019, *ENN* metric increased for Built-up area, Semi forest land, Water body and Green urban areas and decreased for Cropland, Dense forest land and Pastures. ENN value was also predicted to increase in Semi forest land and Dense forest land and decrease in Built-up area, Cropland, and Green urban areas from 2019 to 2039.

From 1999 to 2019, an increase was seen in the *ED* of Built-up area, Dense forest land, Pastures and Green urban areas and a decline in that of Cropland, Semi forest land and Water body. The metric was further predicted to increase in Built-up area and decrease in Cropland, Semi forest land and Dense forest land classes from 2019 to 2039.

The landscape level (*CONTAG*) had an increasing trend from 1999 to 2019. The map of modelling in 2039 also showed a continuous increase of *CONTAG*.

SHDI at landscape level dropped from 1999 to 2019 and was predicted to decrease in 2039.

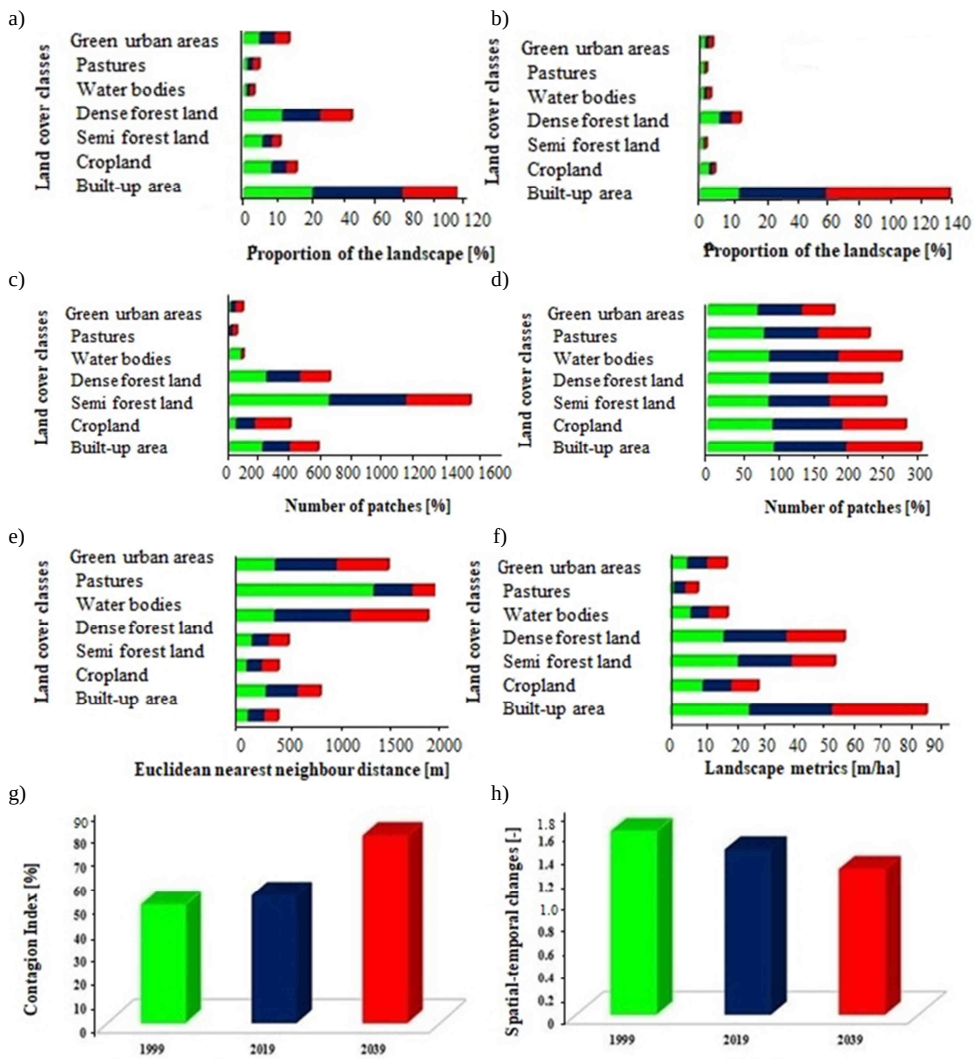


Fig. 10. Changes in Landscape metrics in ■ - 1999, ■ - 2019 and ■ - 2039: a) *PLAND*, b) *LPI*, c) *NP*, d) *IJI*, e) *ENN*, f) *ED*, g) *CONTAG* and h) *SHDI*

Discussion

How does urban expansion influence land use change?

Urban expansion is one of the most important human factors that directly and indirectly influence the land use change through altering the landscape patterns [29]. The changes have led to the wide conversion of land uses from Cropland, Semi forest land and Dense forest land into Built-up area. As the results indicate, the area occupied by Built-up class is predicted to increase in 2039, as it did in 2019. However, the Cropland, Semi forest land and Dense forest land will decrease in 2039, as it declined in 2019. The Water body class did not remarkably changed in the three mentioned years, while Green urban areas gradually decreased in 2039, as it dropped in 2019. The Pastures showed an increase in 2019 and no change in 2039. The land cover prediction for 2039 (Fig. 8) showed a decline in the Cropland, Semi forest land and Dense forest land areas, mainly in the northeastern and eastern regions, together with the fragmentation of the Dense forest land areas (central region) and an expansion of Built-up area to the east and northwest. For 2039, an increase was observed in the Built-up area of the eastern region due to the decrease in the Dense forest land class and Cropland.

In the northwest region, the Cropland and Green urban areas decreased and were replaced by the Built-up area class. Based on the findings, Built-up area would expand over Semi forest land and Dense forest land and convert a large proportion of them into urban land, indicating that the tendency of Vilnius city for urban expansion is increasing. The effects of urban growth often create challenges for planners and policymakers. The spatial modelling process of future urban growth in the Vilnius city can be potentially beneficial in various domains. For example, it helps determine spatiotemporal patterns and trends of growth and simulate interactions between urban development and surrounding landscape [42]. The dynamic of Built-up areas is correlated with urban population growth [42, 52] resulted from higher fertility and rural-urban migration. Therefore, the increasing tendency for the expansion of urban agglomerations is firstly linked with the increase in the future population. The simulation results indicated that 13.29 km^2 will be added to the Built-up area of Vilnius city in 2039. Lack of appropriate planning policies may cause urban sprawl, and accordingly, destruct vegetation cover and open spaces. The present study is in agreement with the previous studies in that urban expansion related to dramatic changes in the land use may directly and indirectly damage ecosystems [51, 53-55]. The modelling map in the present study shows that the urban expansion of the Vilnius city is inevitable in 2039, although its intensity can be mitigated. As the results showed, forest ecosystems can be influenced by urbanization. This results confirms other findings [42, 51, 53-55].

About 10 km^2 of the total forest area (Semi forest land and Dense forest land) may likely be urbanized in 2039. The change in the coverage of natural ecosystems due to the urbanization in the Vilnius will still affect landscape fragmentation, habitat loss, and local climate changes.

How does urban expansion impact landscape patterns?

The relationship between landscape metrics and urbanization dynamics has been previously studied by many researchers [24, 26, 29, 30, 56, 57].

The increase in population, migration and industries in Vilnius is a major driver of change in land use and landscape pattern. *PLAND* metric represents the area composition of

each type of patch in the study area, which is between 0 and 100. The values closer to 0 indicate a drop in the patch type across the whole landscape and 100 demonstrates that the entire landscape is covered by the patch type. The *PLAND* value of Built-up area significantly increased from 38.7 in 1999 to 50.6 in 2019. Built-up area has covered the highest percentage of the area of Vilnius city since 2019 and will further increase to 60.5 in 2039 based on the simulations.

LPI, as an indicator of landscape fragmentation [57], sharply declined in the Semi forest land, Dense forest land and Green urban areas and increased in the human-made class. The metric decreased in the study areas as a result of rapid urbanization. The largest patch index (*LPI*) in 1999 in Built-up area class was 16.97 %, while it was predicted to amount to 53 % by 2039. *IJI*, as an aggregation metric, is one of the main indexes that describe the landscape spatial pattern [7]. *IJI* metric in Built-up area researched from 83.62 in 1999, to 91.36 in 2019 and to 93.67 in 2039, indicating the increase in the number of adjacent patch types. The rise in IJI and LPI increased the probability of territorial urbanization. These two metrics are the determinant of landscape distribution and diversity of plant species [58]. The decreased number of patches in Built-up area, Semi forest land, Dense forest land and Water bodies is caused by the increase in their size and integration from 1999 to 2039. The increased *LPI* and *IJI* and decreased *NP* in areas with a high probability of urbanization were also reported in [19, 24, 30].

ENN-MN reflects the distance among the Built-up patches, indicating that the time when the patches are farther from each other is the less suitable status for integration [19]. In fact, this metric shows the fragmentation rate of a class. The highest fragmentation rates were observed in 1999, 2019 and 2039 in Pastures and water body classes, respectively. The lowest fragmentation in the three years was related to Semi forest land.

Edge Density (*ED*) is used to evaluate the fragmentation of urbanized landscape. In Built-up areas, this metric increased from 27.29 in 1999 to 28.79 in 2019, which indicates the increased dispersion and irregularity of the Built-up area patches. This metric was predicted to further increase in 2039 (*ED* = 32.6). In Dense forest land, the metric showed an increasing trend, from 18.44 in 1999 to 21.88 in 2019, followed by a decreasing trend to 19.93 in 2035. Cropland and Semi forest land similarly showed a continuous decline of *ED* from 1999 to 2039.

The decrease indicated that urban expansion was resulted from the coalescence of adjacent patches, while the *ED* value of the Water bodies, Pastures and Green urban areas were controlled and remained constant. The value of *CONTAG* ranges from 0 to 100. It gets closer to 0 when patch types are dissociated to the maximum and interleaved and comes close to 100 when all types of patch are added at maximum. This metric has had an increasing trend from 49.88 in 1999, to 53.87 in 2019 and 58.63 in 2039. Therefore, due to the increase in this metric in Vilnius city, the extent fragmentation is confirmed at the overall landscape level.

SHDI is equal to zero when only one patch exists in the landscape. It rises because of the increase in the number of different types of patches and/or higher equitability of the proportional distribution of the area between the different types of patch. *SHDI* is sensitive to the unbalanced distribution of different types of patch within the landscape [59]. The *SHDI* metric decreased from 1.6 in 1999 to 1.4 in 2019. Furthermore, the map of modelling in 2039 showed the continuous decrease of *SHDI* to 1.2. Increased human interference and decreased Shannon index metric showed the decrease in the heterogeneity of land use in Vilnius city. In fact, as the urbanization process increased, *SHDI* decreased

dramatically and made the landscape patches more regular and aggregated. The results are in accordance with that of [30].

In this study there are limitations in the *LCM* model. this method on the are adapted from changes that have taken place in *LULC* from the past to the present and could be used only for generation a Business As Usual scenario for the future. So, in *LULC* studies using this method, conservational scenarios cannot be defined.

Conclusion

The present study aimed to indicate the land cover alterations in Vilnius city and the surrounding areas between 1999 and 2019 in order to understand the future land use scenario of the area through integrating remote sensing and advanced *GIS* techniques with the *ANN* model and Markov model. The landscape metrics was also applied to evaluate the *LULC* dynamics. *PLAND*, *LPI*, *NP*, *IJI*, *ENN* and *ED* in the class level and *CONTAG* and *SHDI* in the landscape level were also used to show the effect of urban expansion on landscape patterns. These advanced tools has been widely used over the recent decades to model land use changes because they provide important, spatially explicit results for analysing complex phenomena such as land use changes and, consequently, land cover dynamics. The *CA-ANN* model presented in this study can be applied to other study cases if linked with *GIS*. As the results showed, the main change of the land cover in 2019 compared with 1999 was the increase in the Built-up area and decrease in the forest (Semi forest and Dense Forest) classes. The predicted scenario for 2039 demonstrated a remarkable increase in the Built-up area which represented about 60 % of the area. The percentage distribution of land cover revealed that about 47 % of the land was under vegetation in 2019, while it will be only 36 % in 2039 if this trend continues further. According to the findings, the major urban expansion occurred across vegetation areas. Therefore, land use change has altered the landscape pattern so that the growth and development of urban lands have resulted in the fragmentation and heterogeneity of the whole landscape.

The results of the present study can provide more information about the urban growth pattern for decision makers and planners and help them in their planning schemes. Geospatial simulation is a technique remarkably applicable in modelling and forecasting the urban growth and its impacts on future planning and sustainable development. Perception of the urban complexities, and conscious awareness and application of the findings of this study to Vilnius city would provide a better policy-making, planning and management response to handle the urban growth or urbanization phenomenon. In addition, the results can act as helpful guideline for planners and local governors to manage the spatiotemporal directions of urban expansion and their future outcomes.

Acknowledgements

This research was performed as part of the employment of the authors at Vilnius Gediminas Technical University as employees and PhD student.

References

[1] United Nations, Department of Economic and Social Affairs, Population Division. World Urbanization Prospects: The 2018 Revision (ST/ESA/SER.A/420). New York: United Nations; 2019. Available from: https://population.un.org/wup/Publications/Files/WUP2018-Report.pdf.

[2] Kyakuno T. Prediction of land use changes with Bayesian spatial modeling from the perspective of urban climate. Urban Climate. 2020;31:100569. DOI: 10.1016/j.uclim.2019.100569.
[3] Homer C, Dewitz J, Jin S, Xian G, Costello C, Danielson P, et al. Conterminous United States land cover change patterns 2001-2016 from the 2016 National Land Cover Database. ISPRS J Photogrammetry Remote Sensing. 2020;162:184-99. DOI: 10.1016/j.isprsjprs.2020.02.019.
[4] Islam K, Rahman F, Jashimuddin M. Modeling land use change using Cellular Automata and Artificial Neural Network: The case of Chunati Wildlife Sanctuary, Bangladesh. Ecol Indicators. 2018;88:439-53. DOI: 10.1016/j.ecolind.2018.01.047.
[5] He Y, Zhang D, Huang X, Zhao Y. Assessing the potential impacts of urban expansion on regional carbon storage by linking the LUSD-urban and InVEST models. Environ Modelling Software. 2016;75:44-58. DOI: 10.1016/j.envsoft.2015.09.015.
[6] Yu W, Zhang Y, Zhou W, Wang W, Tang R. Urban expansion in Shenzhen since 1970s: A retrospect of change from a village to a megacity from the space. Phys Chem Earth. 2019;110:21-30. DOI: 10.1016/j.pce.2019.02.006.
[7] Wang Ch, Wang Y, Wang R, Zheng P. Modeling and evaluating land-use/land-cover change for urban planning and sustainability: A case study of Dongying city, China. J Cleaner Prod. 2018;172:1529-34. DOI: 10.1016/j.jclepro.2017.10.294.
[8] Zhou W, Zhang S, Yu W, Wang J, Wang W. Effects of urban expansion on forest loss and fragmentation in six megaregions, China. Remot Sens. 2017;9:991. DOI: 10.3390/rs9100991.
[9] Salvati L, Lamonica G. Containing urban expansion: Densification vs greenfield development, sociodemographic transformations and the economic crisis in a Southern European City, 2006-2015. Ecol Indicators. 2020;110,105923. DOI: 10.1016/j.ecolind.2019.105923.
[10] Chen Sh, Feng Y, Tong X, Liu S, Xie H, Gao Ch, et al. Modeling ESV losses caused by urban expansion using cellular automata and geographically weighted regression. Sci Total Environ. 2020;712,136509. DOI: 10.1016/j.scitotenv.2020.136509.
[11] Zhou L, Dang X, Sun Q, Wang Sh. Multi-scenario simulation of urban land change in Shanghai by random forest and CA-Markov model. Sust Cities Society. 2020;55:102045. DOI: 10.1016/j.scs.2020.102045.
[12] Karimi Firozjaei M, Sedighi A, Argany M, Jelokhani-Niaraki M, Jokar Arsanjani J. A geographical direction-based approach for capturing the local variation of urban expansion in the application of CA-Markov model. Cities. 2019;93:120-35. DOI: 10.1016/j.cities.2019.05.001.
[13] Mirbagheri B, Alimohammadi A. Improving urban cellular automata performance by integrating global and geographically weighted logistic regression models. Trans GIS. 2017;21:6. DOI: 10.1111/tgis.12278.
[14] Zhong S, Qian Y, Chandan Z, Chun L, Ruby W, Hailong Y, et al. Urbanization effect on winter haze in the Yangtze River Delta region of China. Geophys Res Lett. 2018;13:6710-8. DOI: 10.1029/2018GL077239.
[15] Son N, Chen C, Chen C. Urban expansion and its impacts on local temperature in San Salvador, El Salvador. Urban Climate. 2020;32,100617. DOI: 10.1016/j.uclim.2020.100617.
[16] Luo K, Hu X, He Q, Wu Z, Cheng H, Hu Z, et al. Impacts of rapid urbanization on the water quality and macroinvertebrate communities of streams: A case study in Liangjiang New Area, China. Sci Total Environ. 2018;621:1601-14. DOI: 10.1016/j.scitotenv.2017.10.068.
[17] Xie H, Zhang Y, Duan K. Evolutionary overview of urban expansion based on bibliometric analysis in Web of Science from 1990 to 2019. Habitat Int. 2020;95:102100. DOI: 10.1016/j.habitatint.2019.102100.
[18] Huang Z, Wei Y, He C, Li H. Urban land expansion under economic transition in China: A multi-level modeling analysis. Habitat Int. 2015;47:69-82. DOI: 10.1016/j.habitatint.2015.01.007.
[19] Mohammad A, Worku H. Simulating urban land use and cover dynamics using cellular automata and Markov chain approach in Addis Ababa and the surrounding. Urban Climate. 2020;31:100545. DOI: 10.1016/j.uclim.2019.100545.
[20] Romano G, Abdelwahab O, Gentile F. Modeling land use changes and their impact on sediment load in a Mediterranean watershed. Catena. 2018;163:342-53. DOI: 10.1016/j.catena.2017.12.039.
[21] Xu T, Gao J. Directional multi-scale analysis and simulation of urban expansion in Auckland, New Zealand using logistic cellular automata. Computers, Environ Urban Systems. 2019;78:101390. DOI: 10.1016/j.compenvurbsys.2019.101390.
[22] Zhang J, Hao Y, Hu B, Huo X, Hao P, Liu Z. The effects of monsoons and climate teleconnections on the Niangziguan Karst Spring discharge in North China. Clim Dynam. 2017;48:53-70. DOI: 10.1007/s00382-016-3062-2.
[23] Huilei L, Jian P, Yanxu L, Yina H. Urbanization impact on landscape patterns in Beijing City, China: A spatial heterogeneity perspective, Ecol Indicators. 2017;82:50-60. DOI: 10.1016/j.ecolind.2017.06.032.
[24] Nong D, Lepczyk C, Miura T, Fox J. Quantifying urban growth patterns in Hanoi using landscape expansion modes and time series spatial metrics. PLoS ONE. 2018;13(5):e0196940. DOI: 10.1371/journal.pone.0196940.

[25] Sun X, Crittenden J, Li F, Lu Z, Dou X. Urban expansion simulation and the spatio-temporal changes of ecosystem services, a case study in Atlanta Metropolitan area, USA. Sci Total Environ. 2018;622-623;974-87. DOI: 10.1016/j.scitotenv.2017.12.062.
[26] Armenteras D, Murcia U, Gonzalez T, Baron O, Arias J. Scenarios of land use and land cover change for NW Amazonia: Impact on forest intactness. Global Ecol Conserv. 2019;17:e00567. DOI: 10.1016/j.gecco.2019.e00567.
[27] Tong L, Hu Sh, Frazier A. Hierarchically measuring urban expansion in fast urbanizing regions using multi-dimensional metrics: A case of Wuhan metropolis, China. Habitat Int. 2019;94:102070. DOI: 10.1016/j.habitatint.2019.102070.
[28] Yang Y, Zhang D, Nan Y, Liu Zh, Zheng W. Modeling urban expansion in the transnational area of Changbai Mountain: A scenario analysis based on the zoned land use scenario dynamics-urban model. Sust Cities Soc. 2019;50:101622. DOI: 10.1016/j.scs.2019.101622.
[29] Dadashpoor H, Salarian F. Urban sprawl on natural lands: Analyzing and predicting the trend of land use changes and sprawl in Mazandaran city region, Iran. Environ Development Sust. 2018;22:593-614. DOI: 10.1007/s10668-018-0211-2.
[30] Bonilla-Bedoya S, Mora A, Vaca A, Estrella A, Ángel Herrera M. Modelling the relationship between urban expansion processes and urban forest characteristics: An application to the Metropolitan District of Quito. Computers, Environ Urban Systems. 2020;79:101420. DOI: 10.1016/j.compenvurbsys.2019.101420.
[31] Yang J, LI Sh, Xu J, Wang X, Zhang X. Effects of changing scales on landscape patterns and spatial modeling under urbanization. J Environ Eng Landscape Manage. 2020;28(2): 62-73. DOI: 10.3846/jeelm.2020.12081.
[32] Basse RM, Omrani H, Charif O, Gerber P, Bodis K. Land use changes modelling using advanced methods: Cellular automata and artificial neural networks. The spatial and explicit representation of land cover dynamics at the cross-border region scale. Appl Geography. 2014;53:160-71. DOI: 10.1016/j.apgeog.2014.06.016.
[33] Ansari A, Golabi M. Prediction of spatial land use changes based on LCM in a GIS environment for Desert Wetlands - A case study: Meighan Wetland, Iran. Int Soil Water Conserv Res. 2019;7,64-70. DOI: 10.1016/j.iswcr.2018.10.001.
[34] Silva L, Xavier A, Silva R, Santos G. Modeling land cover change based on an artificial neural network for a semiarid river basin in northeastern Brazil. Global Ecol Conserv. 2020;21:e008112019. DOI: 10.1016/j.gecco.2019-00811.
[35] Isik S, Kalin L, Schoonover J, Srivastava P, Lockaby G. Modeling effects of changing land use/cover on daily streamflow: An Artificial Neural Network and curve number based hybrid approach. J Hydrol. 2013;485:103-12. DOI: 10.1016/j.jhydrol.2012.08.032.
[36] Taraškevičius R, Motiejūnaitė G, Zinkutė R, Eigminienė A, Gedminienė L, Stankevičius Z. Similarities and differences in geochemical distribution patterns in epiphytic lichens and topsoils from kindergarten grounds in Vilnius. J Geochem Explor. 2017;183:152-65. DOI: 10.1016/j.gexplo.2017.08.013.
[37] Geological Survey. Geological Survey Download GLOVIS. Available from: https://glovis.usgs.gov, Accessed 29th Dec 2019.
[38] Mancino G, Ferrara A, Padula A, Nolè A. Cross-Comparison between Landsat 8 (OLI) and Landsat 7 (ETM+) Derived Vegetation Indices in a Mediterranean Environment. Remote Sensing. 2020;12:291. DOI: 10.3390/rs12020291.
[39] Samardžic-Petrovic M, Kova¡cevic M, Bajat B, Dragi'cevic S. Machine learning techniques for modelling short term land-use change. ISPRS Int J Geology-Information. 2017;6:387. DOI: 10.3390/ijgi6120387.
[40] Heydari S, Mountrakis G. Meta-analysis of deep neural networks in remote sensing: A comparative study of mono-temporal classification to support vector machines. ISPRS J Photogrammetry Remote Sensing. 2019;152:192-210. DOI: 10.1016/j.isprsjprs.2019.04.016.
[41] Karimi F, Sultana S, Shirzadi Babakan A, Suthaharan Sh. An enhanced support vector machine model for urban expansion prediction. Computers, Environ Urban Systems. 2019;75:61-75. DOI: 10.1016/j.compenvurbsys.2019.01.001.
[42] Santana EF, Vidal Batista L, Silva RM, Santos CA. Multispectral image unsupervised segmentation using watershed transformation and cross-entropy minimization in different land use. GIScience Remote Sensing. 2014;51(6):613-29. DOI: 10.1080/15481603.2014.980095.
[43] Roohi R, Jafari M, Jahantab E, Saffari Aman M, Moameri M, Zare S. Application of artificial neural network model for the identification the effect of municipal waste compost and biochar on phytoremediation of contaminated soils. J Geochem Exploration. 2020;208:106399. DOI: 10.1016/j.gexplo.2019.106399.
[44] Ray A, Halder T, Jena S, Sahoo A, Ghosh B, Mohanty S, et al. Application of artificial neural network (ANN) model for prediction and optimization of coronarin D content in Hedychium coronarium. Industrial Crops Products. 2020;146:112186. DOI: 10.1016/j.indcrop.2020.112186.

[45] Liu X, Zhu X, Zhang Q, Yang T, Pan Y, Sun P. A remote sensing and artificial neural network-based integrated agricultural drought index: Index development and applications. Catena. 2020;186:104394. DOI: 10.1016/j.catena.2019.104394.
[46] Thangavel R, Kanchikerimath M, Sudharsanam A, Ayyanadar A, Karunanithi R, Deshmukh N, et al. Evaluating organic carbon fractions, temperature sensitivity and artificial neural network modeling of CO_2 efflux in soils: Impact of land use change in subtropical India (Meghalaya). Ecol Indicators. 2020;93:129-41. DOI: 10.1016/j.ecolind.2018.04.077.
[47] Nasiri V, Darvishsefat A, Rafiee R, Shirvany A, Hemat M. Land use change modeling through an integrated Multi-Layer Perceptron Neural Network and Markov Chain analysis (case study: Arasbaran region, Iran). J Forestry Res. 2018;30(3):943-57. DOI: 10.1007/s11676-018-0659-9.
[48] Shooshtarian M, Dehghani M, Margherita F, Gea O, Mortezazadeh Sh. Land use change and conversion effects on ground water quality trends: An integration of land change modeler in GIS and a new Ground Water Quality Index developed by fuzzy multi-criteria group decision-making models. Food Chem Toxicol. 2019;114:204-14. DOI: 10.1016/j.fct.2018.02.025.
[49] Hamdy O, Zhao S, Salheen M, Eid Y. Analyses the driving forces for urban growth by using IDRISI Selva Models Abouelreesh - Aswan as a case study. Int J Eng Technol. 2017;9(3):226-32. DOI: 10.7763/IJET.2017.V9.975.
[50] Zarandian A, Baral H, Stork N, Ling M, Yavari A, Jafari H, et al. Modeling of ecosystem services informs spatial planning in landsadjacent to the Sarvelat and Javaherdasht protected area in northern Iran. Land Use Policy. 2017;61:487-500. DOI: 10.1016/j.landusepol.2016.12.003.
[51] Su S, Xiao R, Jiang Z, Zhang Y. Characterizing landscape pattern and ecosystem service value changes for urbanization impacts at an eco-regional scale. Appl Geogr. 2012;34:295-305. DOI: 10.1016/j.apgeog.2011.12.001.
[52] You H. Agricultural landscape dynamics in response to economic transition: comparisons between different spatial planning zones in Ningbo region, China. Land Use Policy. 2017;61:316-28. DOI: 10.1016/j.landusepol.2016.11.025.
[53] Wu K, Ye X, Qi Z, Zhang H. Impacts of land use/land cover change and socioeconomic development on regional ecosystem services: the case of fast-growing Hangzhou metropolitan area, China. Cities. 2013;31:276-84. DOI: 10.1016/j.cities.2012.08.003.
[54] Long H, Liu Y, Hou X, Li T, Li Y. Effects of land use transitions due to rapid urbanization on ecosystem services: implications for urban planning in the new developing area of China. Habitat Int. 2014;44:536-44. DOI: 10.1016/j.habitatint.2014.10.011.
[55] Tripathi R, Moharana K, Nayak A, Dhal B, Shahid M, Mondal B, et al. Ecosystem services in different agro-climatic zones in eastern India: impact of land use and land cover change. Environ Monit Assess. 2019;191(2):98. DOI: 10.1007/s10661-019-7224-7.
[56] Almeida D, Rocha J, Neto C, Arsénio P. Landscape metrics applied to formerly reclaimed saltmarshes: A tool to evaluate ecosystem services? Estuarine, Coastal Shelf Sci. 2016;181:100-13. DOI: 10.1016/j.ecss.2016.08.020.
[57] Hassan MM. Monitoring land use/ land cover change, urban growth dynamics and landscape pattern analysis in five fastest urbanized cities in Bangladesh. Remote Sensing Applications: Society Environ. 2017;7:69-83. DOI: 10.1016/j.rsase.2017.07.001.
[58] Forman R. Urban Ecology: Science of Cities. Cambridge University Press; 2014. ISBN: 9780521188241 DOI: 10.5860/choice.190738.
[59] McGarigal K. Fragstats Help. Amherst: University of Massachusetts. USA; 2015. ISBN: 6450061768432. DOI: umass.edu/landeco/research/fragstats/fragstats.html.